Dispersion Analysis of Magnesium Stannide Reflectivity

HERBERT G. LIPSON AND ALFRED KAHAN
Air Force Cambridge Research Laboratories, Office of Aerospace Research, L. G. Hanscom Field, Bedford, Massachusetts
(Received 9 January 1967)

The optical reflectivity of Mg_2Sn measured between 10 and 45 μ at temperatures of 80, 296, and 473°K shows the effects of both lattice-vibration and free-carrier absorption. For the range of carrier concentrations investigated, 10^{17} to 10^{19} cm^{-3}, the plasma edge, broadened by the short relaxation time of the carriers, occurs on both sides of the transverse-optical lattice frequency, and the effects of both absorption mechanisms are superimposed. Values for the lattice dispersion parameters and carrier effective masses and relaxation times are obtained from the best fit to the experimental reflectivity curves. The relative contribution of the two mechanisms to the total reflectivity is illustrated for a heavily doped Mg_2Sn sample at low temperature; in addition, the masking of the lattice vibration reflectivity as a function of free-carrier concentration and relaxation time is discussed.

I. INTRODUCTION

THE important contributions to the dispersion of optical reflectivity of a semiconductor in the infrared for energies less than the forbidden gap arise from either the fundamental lattice vibration of the crystal or the absorption of free carriers. In order to reduce the reflectivity spectrum to sets of parameters, it is customary to analyze the lattice contribution by classical oscillator theory and to treat the free-carrier absorption in terms of the effective masses and relaxation times of the carriers. The optical reflectivity of magnesium stannide, a compound semiconductor of the II–IV series, measured[1] between 10 and 50 μ as a function of temperature and intrinsic carrier concentration, shows the effects of both of these mechanisms.

Depending on the carrier concentration and effective mass value, the free-carrier plasma edge can occur on either side of the lattice resonance frequency. The sharpness of the edge will be a function of the relaxation time τ. For a long relaxation time material, such as n-type InSb,[2] GaAs,[3] and ZnO,[4] the reflectivity variation with frequency in the neighborhood of the plasma minimum is characterized by one parameter, the effective mass. For materials with short relaxation times, such as p-type Ge, Si, and InSb,[2] the plasma edge increases monotonically with wavelength and the reflectivity is a function of both the effective mass and relaxation time. In these semiconductors, particularly for heavily doped n-type samples the effects of the lattice and free-carrier absorption are separated as a function of frequency, and the parameters have been determined with reasonable accuracy.

Previous measurements[5] made on a relatively pure sample of Mg_2Sn established the wave number of the transverse-optical lattice vibration at room temperature as 186 cm^{-1}. In this investigation the plasma edge occurs on either side of ν_1, but as a consequence of the short relaxation time the effects of the two mechanisms are superimposed for all carrier concentrations. It is the purpose of this paper to interpret the experimental reflectivity data, and to obtain both the lattice and free carrier parameters from the best fit to the experimental reflectivity curves.

II. EXPERIMENTAL PROCEDURES AND RESULTS

The experimental reflectivity values were obtained from direct comparison of the sample reflectivity with that of an evaporated Al mirror, at an 8° angle of incidence. The exit beam of a Perkin-Elmer double pass spectrometer equipped with NaCl, CsBr, and CsI prisms was focussed at a sample position inside an evacuated dewar and the reflected beam from either the sample or the Al mirror was detected by a Reeder CsI window thermocouple. Reflection scanning of both the sample and mirror was performed by moving the dewar in the plane of the spectrometer slit image.

Measurements were made between liquid-nitrogen temperature and approximately 200°C in the same dewar without repositioning the sample or the mirror. Dewar windows of KRS5 (thallium bromide-iodide) or polyethylene were used in the appropriate spectral regions. Short wavelength radiation was eliminated with a LiF reflector in the CsBr prism range and with either a CaF_2 or NaCl reflector used in combination with a black polyethylene transmission filter in the CsI prism range.

The reflectivity studies were performed at 80, 296, and 473°K. Figure 1 shows the carrier concentrations as a function of temperature as determined from Hall effect measurements for the Mg_2Sn samples investigated. At 80°K, all samples are extrinsic with 5×10^{18} holes/cm^3 for the p-type and 3×10^{16}, and 2×10^{18} electrons/cm^3 for the n-type materials. At 296°K, intrinsic ionization is the dominant mechanism for the

[1] H. G. Lipson and A. Kahan, Bull. Am. Phys. Soc. **10**, 593 (1965).
[2] W. G. Spitzer and H. Y. Fan, Phys. Rev. **106**, 882 (1957).
[3] W. G. Spitzer and J. M. Whelan, Phys. Rev. **114**, 59 (1959).
[4] R. J. Collins and D. A. Kleinman, J. Phys. Chem. Solids **11**, 190 (1959).
[5] A. Kahan, H. G. Lipson, and E. V. Loewenstein, in *Proceedings of the International Conference on Physics of Semiconductors* (Dunod Cie., Paris, 1964), p. 1067.

n-type MZ-36, while even at 473°K the other samples are still characterized by mixed conduction. Complete reproducibility of electrical measurements could not be obtained at all temperatures, due to the small size and possibly the surface condition of the samples.

Figures 2, 3, and 4 show the experimental reflectivity data, extending from approximately 220 cm^{-1} to 1000 cm^{-1}, taken at 80, 296, and 473°K, respectively, for samples with the various free-carrier concentrations. Reflectivity curves obtained by dispersion analysis, covering the experimental range and extending to 10 cm^{-1}, are also shown in these figures. For the purest material MZ-36 at the lowest temperature the lattice vibration is the dominant mechanism and the reflectivity follows the behavior of a typical polar semiconductor lattice. As the free-carrier concentration is increased, the reflectivity curves begin to represent the combined effects of lattice vibration and free-carrier absorption with the masking of the lattice vibration more pronounced at higher densities. This superposition occurs either for a particular sample as carriers are ionized with increasing temperature, or for different samples with a range of concentrations at the same temperature. However, owing to the temperature shift of the lattice vibration, identical carrier densities at different temperatures will not lead to the same reflectivity curve. The dip in the experimental values for MZ-36 at 80°K in the 320 to 360 cm^{-1} range is attributed to two phonon combination bands. We have also observed these bands in transmission for thinner samples of this material.

III. ANALYSIS

Classical oscillator analysis of lattice vibration reflectivity and the free-carrier contribution to the susceptibility, considered as a resonance at $\nu=0$, has been extensively reviewed and discussed.[6–9] The equations for the real and imaginary parts of the complex dielectric constant, using notation similar to Sanderson's,[10] are

$$\epsilon'=n^2-k^2=\epsilon_\infty+\sum_j \frac{(4\pi\rho_j\nu_j^2)(\nu_j^2-\nu^2)}{(\nu_j^2-\nu^2)^2+(\gamma_j\nu_j\nu)^2}-\frac{A}{\nu^2+G^2} \quad (1a)$$

and

$$\epsilon''=2nk=\sum_j \frac{(4\pi\rho_j\nu_j^2)(\gamma_j\nu_j\nu)}{(\nu_j^2-\nu^2)^2+(\gamma_j\nu_j\nu)^2}+\frac{AG}{\nu(\nu^2+G^2)}, \quad (1b)$$

while the reflectivity at the normal angle of incidence is calculated from

$$R=[(n-1)^2+k^2]/[(n+1)^2+k^2]. \quad (2)$$

[6] F. Stern, in *Solid State Physics*, edited by F. Seitz and D. Turnbull (Academic Press Inc., New York, 1963), Vol. 15, p. 351.
[7] E. Burstein, *Phonon and Phonon Interactions* (W. A. Benjamin, Inc., New York, 1964), p. 276.
[8] J. R. Jasperse, A. Kahan, J. N. Plendl, and S. S. Mitra, Phys. Rev. **146**, 526 (1966).
[9] T. S. Moss, *Optical Properties of Semiconductors* (Butterworths Scientific Publications Ltd., London, 1959), p. 15.
[10] R. B. Sanderson, J. Phys. Chem. Solids **26**, 803 (1965).

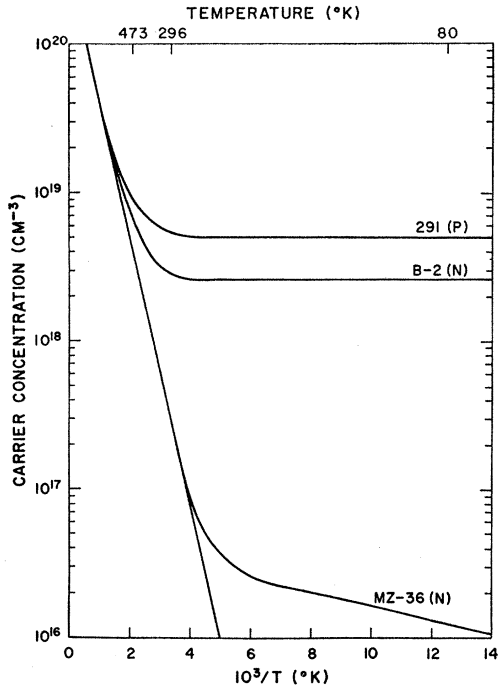

FIG. 1. Carrier concentration as a function of temperature for Mg_2Sn samples.

In these equations, n is the refractive index, k the extinction coefficient, ϵ_∞ the high-frequency dielectric constant, $4\pi\rho_j$ the strength, γ_j the damping constant, and ν_j the frequency of the jth resonance. The carrier effective mass and relaxation time τ(sec) are defined in terms of the free carrier parameters A (cm^{-2}) and G (cm^{-1}) as

$$m^*/m_e=e^2N/m_ec^2\pi A=8.97\times10^{-14}N/A \quad (3)$$

and

$$\tau=1/2\pi cG=5.31\times10^{-12}/G, \quad (4)$$

where m_e is the electronic mass, and N the carrier density in cm^{-3}. The details of the classical analysis computer program, modified for the present study to include free-carrier effects, were given in a previous report.[11]

Six parameters are required to describe the reflectivity spectrum of a one-resonance lattice vibration combined with absorption of one type of free carrier. If both electrons and holes contribute to the absorption process, then in Eqs. (1a) and (1b), two terms, one for each type of carrier, are included and the reflectivity curve is determined by eight parameters. It is highly unlikely that six or eight parameters can be uniquely evaluated from the analysis of a single reflectivity experiment, particularly for carriers with short relaxation times. To minimize these difficulties, there exist several checks for consistency which one can apply. In our experi-

[11] A. Kahan, Air Force Cambridge Research Laboratories Report No. 66-327, 1966 (unpublished).

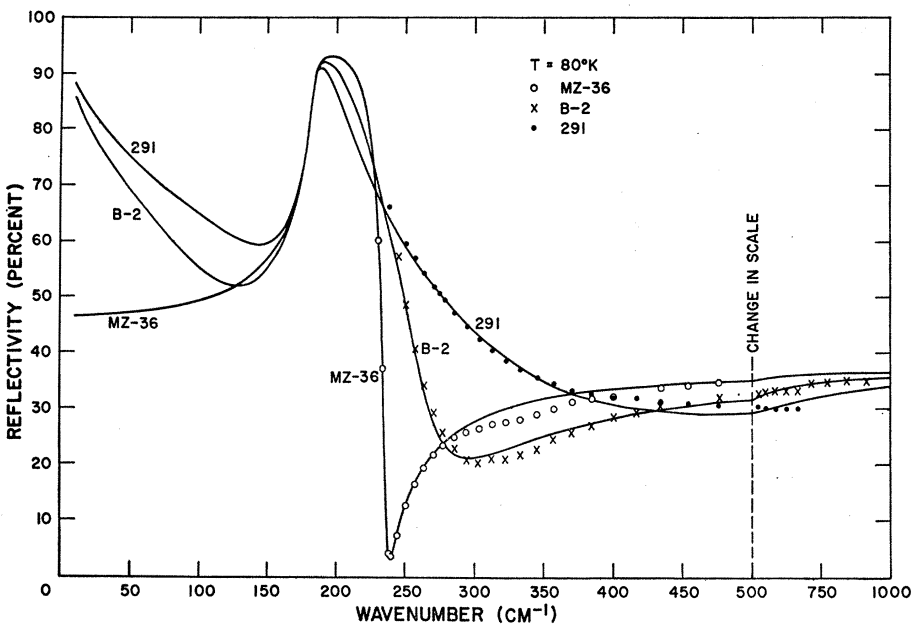

FIG. 2. Mg_2Sn reflectivity as a function of wave number at 80°K. The experimental points are represented by the various symbols and the solid curves were calculated from the dispersion parameters given in Table I.

ments, the reflectivity spectrum of three samples with different carrier concentrations were measured and as the first constraint, the criterion of fitting all curves at a particular temperature with identical lattice parameters is applied. In addition, one expects a continuous variation of the lattice parameters as a function of temperature. In the case of the free-carrier parameters, only those values of A which yield a constant or smoothly varying effective mass as a function of carrier concentration should be considered. Likewise, the relaxation time calculated from G should show a correlation with carrier mobilities determined from electrical measurements.

The question of accuracy of the calculated lattice and free-carrier parameters has to be examined. Can the value of each parameter be determined uniquely from a particular segment of the reflectivity spectrum, or are more than one of the parameter values influenced by the same region, and as a consequence will the simultaneous change of two parameters yield the same curve? The uniqueness of the parameter values will be different depending on whether the reflectivity is determined solely by the lattice vibration or by a superposition of the lattice and free carriers. In this respect we consider the parameter values of the MZ-36 and 291 samples at 80°K tabulated in the next section.

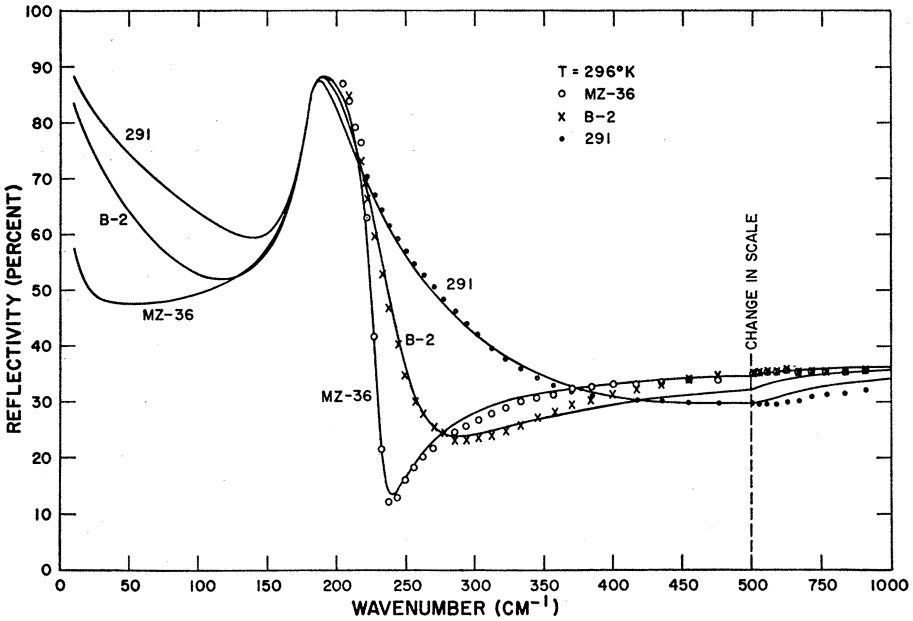

FIG. 3. Mg_2Sn reflectivity as a function of wave number at 296°K. The experimental points are represented by the various symbols and the solid curves were calculated from the dispersion parameters given in Table I.

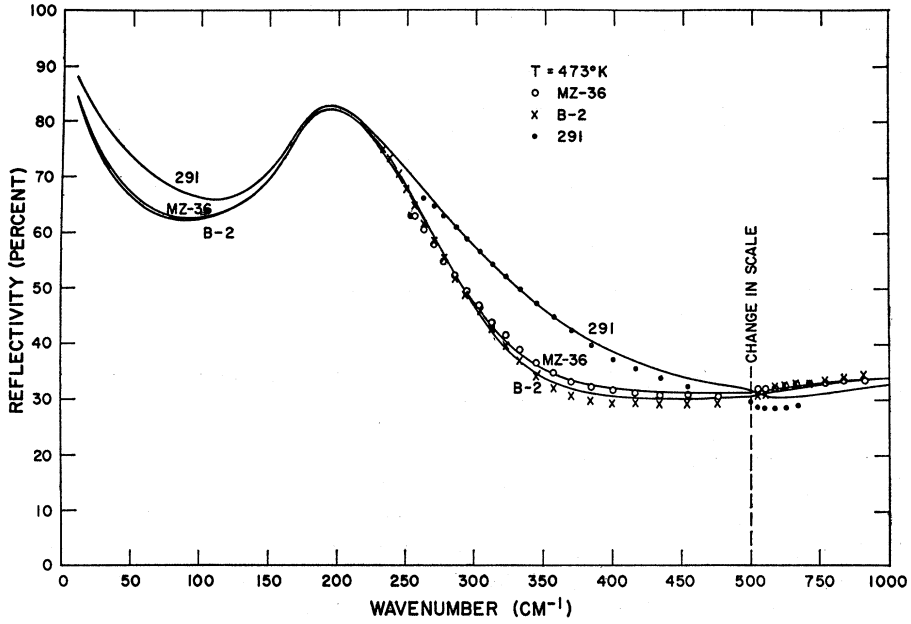

FIG. 4. Mg_2Sn reflectivity as a function of wave number at 473°K. The experimental points are represented by the various symbols and the solid curves were calculated from the dispersion parameters given in Table I.

We perform a variation of each parameter value, one at a time, of magnitude comparable to the experimental accuracy, so that either the resulting maximum change in reflectivity will be less than 0.02 in the flat regions, or the maximum wave number displacement will not exceed 3 to 4 cm^{-1} in the steep regions of the spectra. It is found that fitting the reflectivity spectrum of MZ-36, a one-resonance lattice vibration, uniquely, is a relatively simple procedure. The near-infrared reflectivity level determines ϵ_∞, the far-infrared value establishes $4\pi\rho_1$, the position of the low frequency side of the resonance band determines ν_1, and the maximum reflectivity value governs γ_1.

The introduction of free carriers adds the additional two parameters A and G, and matters become more complicated. The results of this study are illustrated in Figs. 5(a)–5(f). The solid line in all cases corresponds to the basic curve; dotted the lines depict the variations on a three times expanded scale. As in the case of pure lattice vibration, ϵ_∞ can still be established from the near-infrared level, as seen in Fig. 5(a), and ν_1 from the position of the low-frequency side of the resonance band, as indicated in Fig. 5(b). However, free carriers dominate the far-infrared reflectivity and $4\pi\rho_1$ can no longer be deduced from this region. Similarly, the maximum reflectivity value is equally influenced by two lattice

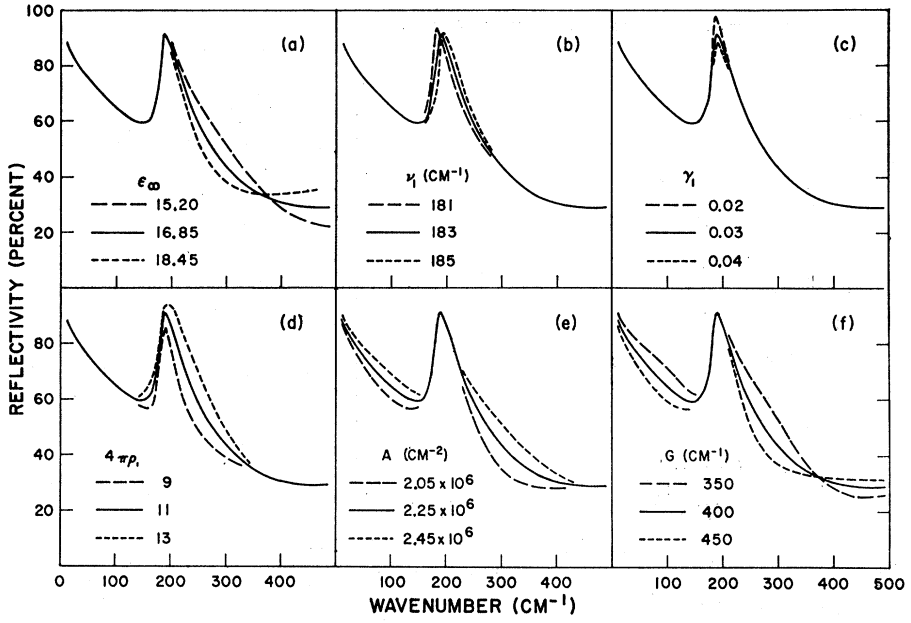

FIG. 5. Variation of reflectivity parameters. The solid curve in each figure corresponds to the reflectivity of sample 291 at 80°K, whose parameters are listed in Table I. The dotted curves represent the effect of variation of individual parameters. The deviations from the solid curve are expanded by a factor of 3.

TABLE I. Lattice and free-carrier parameters of Mg_2Sn samples.[a]

Temperature °K	Lattice parameters ν_1 cm^{-1}	γ_1	$4\pi\rho_1$		Free-carrier parameters for sample number MZ-36	B-2	291
80	183	0.03	11.0	A (cm^{-2})	...	7.25×10^5	2.25×10^6
				G (cm^{-1})	...	200	400
296	180	0.05	11.0	A (cm^{-2})	3.00×10^5	7.25×10^5	2.25×10^6
				G (cm^{-1})	875	275	425
473	177	0.20	28.5	A (cm^{-2})	3.35×10^6	2.70×10^6	3.80×10^6
				G (cm^{-1})	1050	900	700

[a] $\epsilon_\infty = 16.85$ ($R_\infty = 0.37$) at all temperatures.

parameters and this precludes the unique determination of γ_1. It can be noted from Figs. 5(d), 5(e), and 5(f) that the effects of $4\pi\rho_1$, A, and G overlap the same spectral region, and identical reflectivity curves can result from a systematic shift of a combination of these parameters.

A complete analysis would proceed to establish the lattice parameters from a pure sample and distinguish between A and G by a judicious choice of experimental conditions, sample doping, and the additional consistency checks previously outlined. Independent measurements, if available, of either the lifetime or of the effective mass will simplify the analysis.

IV. DISCUSSION

The parameter values obtained from the best fit of the available experimental points, consistent with the constraints outlined in the previous section, are given in Table I, and the calculated reflectivity curves are shown in Figs. 2, 3, and 4. Within the limits of experimental accuracy, reasonable agreement is achieved for all samples at all temperatures. With the prism spectrometer used for these measurements, reflection spectra could be obtained only to 220 cm^{-1}; the computed curves however are extended to 10 cm^{-1}. The free-carrier and lattice parameters affect different regions of the reflectivity spectrum to varying degrees, and consequently the lack of far-infrared data introduces uncertainties in some parameter values.

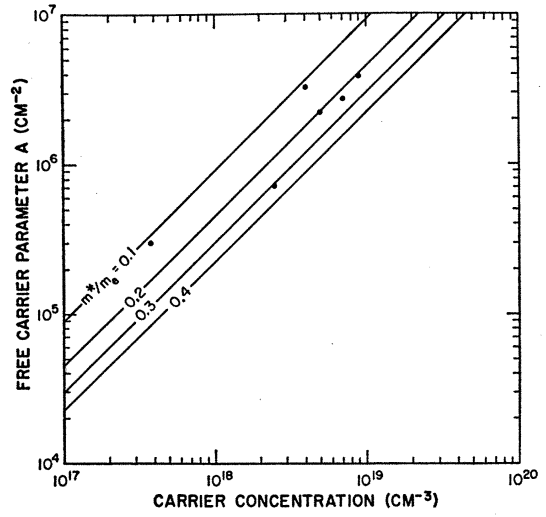

FIG. 6. Free-carrier parameter A as a function of carrier concentration. The solid lines are plots of Eq. (3), and the dots are values, as listed in Table I, determined from the best fit to the experimental reflectivity curves.

The temperature dependence of the lattice constants can be inferred from the listings of Table I. The major criterion applied in setting these values was whether, at a particular temperature, all three of the samples investigated could be fitted with the identical set of dispersion parameters. In a previous publication,[5] room temperature experimental data extended to 100 cm^{-1} were analyzed in terms of a two-resonance lattice model, without considering free-carrier contributions. In the present study, for simplicity, a one-resonance lattice model is assumed, as the effects of the second oscillator are mainly manifested below 220 cm^{-1}. Thus, a direct comparison between the two sets of values is not meaningful, and additional experiments on both pure and doped samples extending beyond the lattice resonance region into the far-infrared are necessary for an accurate determination of the lattice constants and their temperature dependencies.

The values of the free-carrier parameters are also listed in Table I. It was possible to fit all experimental curves based on a one-carrier model. This model is valid in the extrinsic range, and the effective masses of both the electrons and holes can be evaluated from the n- and p-type sample reflectivity data, respectively. For this analysis, as the ratio of the minority to majority carriers is increased, a two-carrier model has to be considered. Neglecting the variation on m^* with N, the computations can be simplified by using the values of m^* found from the extrinsic concentration data. The curve-fitting procedure will then involve establishing the relaxation times of the two types of carriers. Equal or near-equal carrier concentrations do not necessarily imply a two-carrier model, as the relative contribution of the two carriers to the dielectric constant is also affected by the effective mass and relaxation time values of electrons and holes. For Mg_2Sn, the free-carrier parameter A yields electron and hole effective masses of the same order of magnitude, and the justification of a one-carrier model at the higher temperatures, where

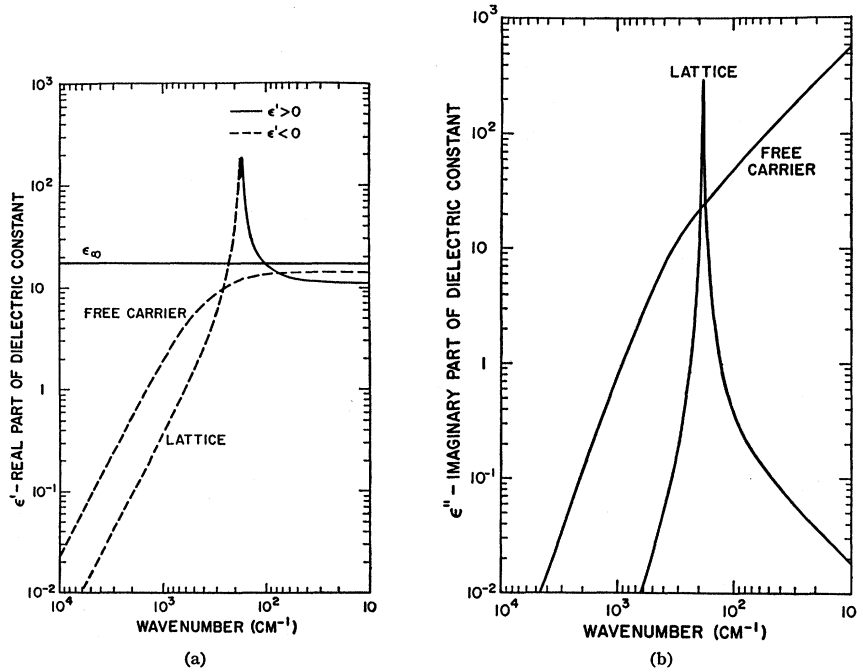

FIG. 7. Calculated real (a) and imaginary (b) parts of the dielectric constant as a function of wave number. The lattice and free-carrier parameters are those of sample 291 at 80°K.

nearly intrinsic conditions exist, will depend on the relative values of the relaxation times. If τ_e and τ_h are widely separated, then the free-carrier parameters of Table I represent only one of the carriers while for approximately equal τ's, the free-carrier parameters are some sort of an average value. Our experimental curves do not justify such a detailed analysis.

Equation (3) gives the relationship between parameter A, effective mass m^*, and carrier concentration N, and the straight lines in Fig. 6 are plots of this equation for constant values of effective mass. Using the concentration of the majority carrier only, m_c^* and m_h^* were calculated from the free-carrier parameters obtained from the best fit to the experimental data, and these values are also shown in Fig. 6. The one-carrier model, which is valid for the low-temperature data, indicates an electronic effective mass of $0.3m_e$ and a hole effective mass of $0.2m_e$. Regardless of the question of the one- or two-carrier model, all calculated values lie in the range of 0.1 to 0.3. Since the computer calculated curves indicate significant differences as a function of carrier concentration between the n- and p-type samples

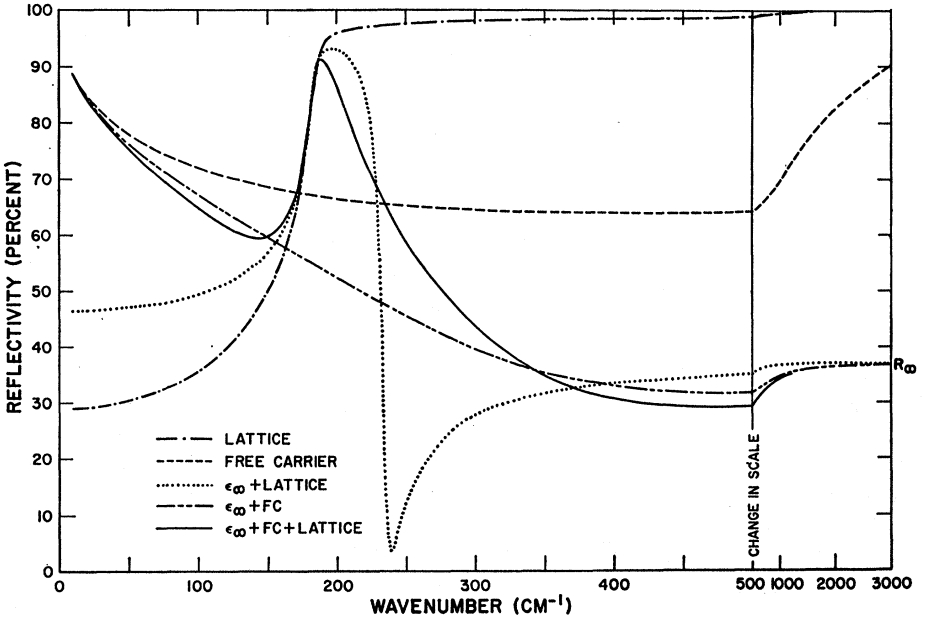

FIG. 8. Calculated reflectivity as a function of wave number for combinations of various absorption mechanisms. Dispersion parameters are those of sample 291 at 80°K.

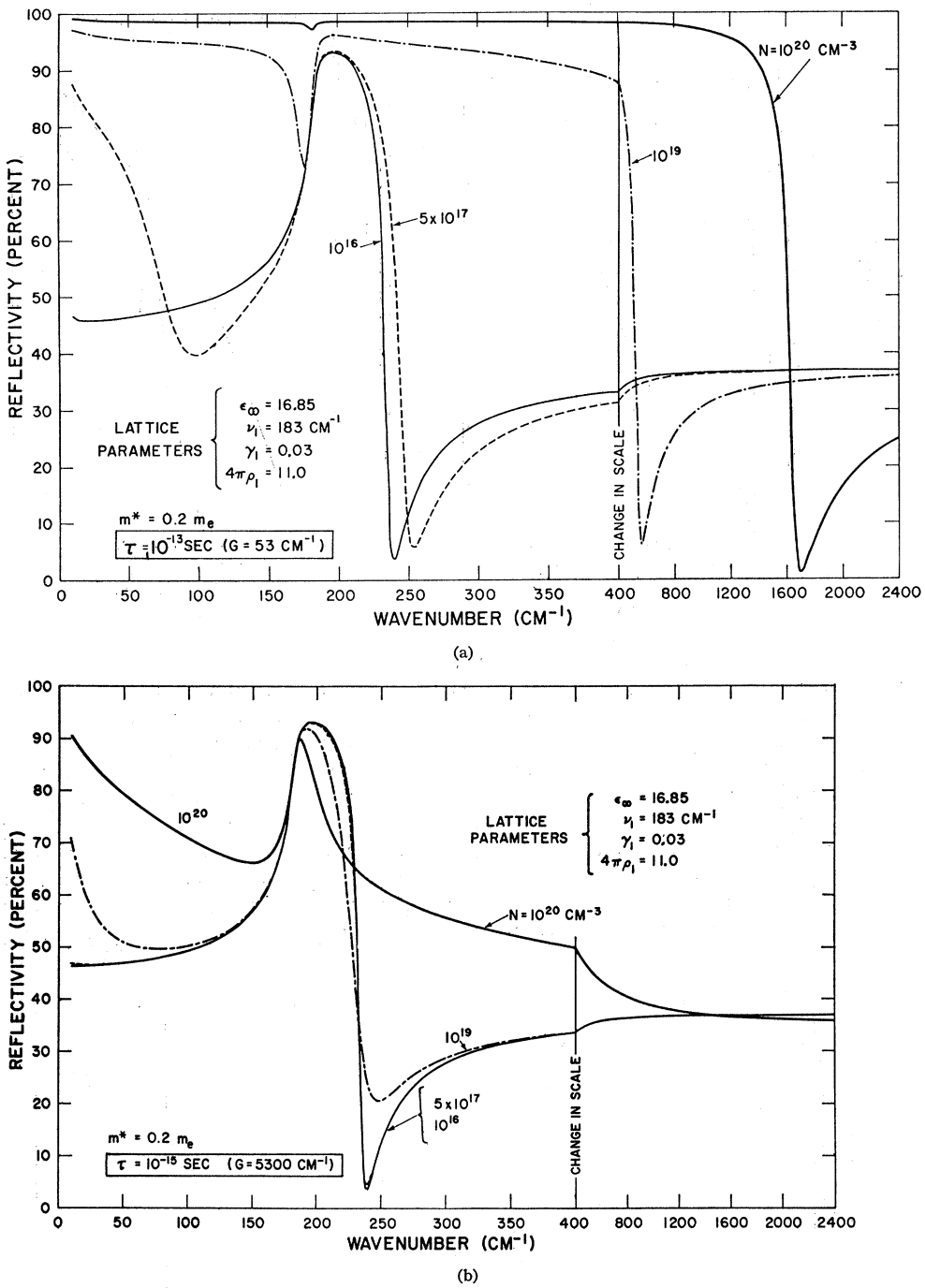

FIG. 9. Calculated reflectivity as a function of wave number for various carrier concentrations and relaxation times of 10^{-13} and 10^{-15} sec.

on the long wavelength side of the lattice vibration, a further test on the accuracy of these values may be obtained from fitting experimental data of this spectral region.

Reflectivity measurements between 50 and 380 cm^{-1} for a range of temperatures have been reported by Geick, Hakel, and Perry.[12] The general characteristics of these curves are similar to the ones shown in Figs. 2, 3, and 4, but due to the absence of carrier concentration measurements no direct comparison can be made between the two sets of data. The classical dispersion-formula fit shown in Ref. 12 has been accomplished by considering a two-carrier model and consequently the fitting of each curve involves eight parameters. As previously discussed, it is highly questionable that for this material which possesses both a short relaxation

[12] R. Geick, W. J. Hakel, and C. H. Perry, Phys. Rev. 148, 824 (1966).

time and superposition of lattice and free-carrier effects, eight parameters can be uniquely determined from the measurement of a single sample.

It is of interest to illustrate the individual contributions of the lattice resonance and free carrier terms to the reflectivity. As a typical example, we select sample 291 at $T=80°K$. The calculated real and imaginary parts of the complex dielectric constant are shown in Fig. 7(a) and 7(b). At low wave numbers, the value of the real part of the dielectric constant of the lattice is positive, has a maximum at $\nu=\nu_1(1-\gamma_1)^{1/2}$, becomes negative at $\nu=\nu_1$, has a minimum at $\nu=\nu_1(1+\gamma_1)^{1/2}$, and follows a $4\pi\rho_1\nu_1^2/\nu^2$ dependence in the high wave number limit. For the free carriers, ϵ' is always negative, varies as A/ν^2 when $\nu\gg G$ (corresponding to $\omega\tau\gg1$) and approaches A/G^2 in the limit when $G\gg\nu$. The value of the imaginary part of the dielectric constant is always positive and possesses a sharp resonance at $\nu=\nu_1$ for the lattice oscillation, while the functional dependence of the free carriers is AG/ν^3 in the $\nu\gg G$ and $A/G\nu$ in the $G\gg\nu$ limit, respectively.

The resulting reflectivity spectra as a function of wave number are shown in Fig. 8. Curve 1 is the reflectivity owing to the one-resonance lattice without any ϵ_∞ contribution. Its major characteristic is to rise to near unity in the region of the resonance frequency, and metallic behavior above the resonance frequency. Curve 2 represents the free-carrier reflectivity which reaches a broad minimum near $\nu=G$ and increases to unity at both ends of the spectrum. The addition of the static dielectric constant, $\epsilon_\infty=16.85$, drastically modifies both reflectivity curves. For the free-carrier absorption, the effect of ϵ_∞ is to chance ϵ' into a positive quantity at all frequencies, whereas the lattice vibration ϵ' will remain negative only in the narrow region near the resonance frequency. The resultant reflectivities are plotted in curves 3 and 4. The former is identical with the MZ-36 low-temperature curve, while the latter is typical for that of carriers with short relaxation time. In this particular case, $m^*=0.2m_e$ and $\tau=1.3\times10^{-14}$ seconds. The superposition of the static dielectric constant, lattice vibration, and free-carrier absorption yields curve 5, that of sample 291 at 80°K.

It is also instructive to consider the gradual masking of the lattice vibration reflectivity as a function of relaxation time and carrier concentration. We consider a semiconductor with lattice parameters, characteristic of Mg_2Sn at $T=80°K$, an effective mass $m^*=0.2m_e$ and with carrier densities varying between 10^{16} cm^{-3} and 10^{20} cm^{-3}. The calculated reflectivities corresponding to a relatively long relaxation time $\tau=10^{-13}$ sec ($G=53$ cm^{-1}) are plotted in Fig. 9(a); those for a short relaxation time $\tau=10^{-15}$ sec ($G=5300$ cm^{-1}) are depicted in Fig. 9(b). For the material with the long relaxation time, and carrier concentration of 10^{16} cm^{-3}, the reflectivity is dominated by the lattice vibration mechanism. As N is increased to 5×10^{17} cm^{-3}, the plasma edge appears around 100 cm^{-1}, but the effects of the two mechanisms are still clearly separable as a function of frequency. At $N=10^{19}$ cm^{-3}, the reflectivity minimum has shifted to approximately 500 cm^{-1} and the lattice vibration is almost completely masked by free-carrier effects. A further increase of N to 10^{20} cm^{-3} shifts the minimum to even longer frequencies while the lattice contribution is nearly imperceptible. These curves are calculated with the value of $m^*=0.2m_e$ but, as evident from the proportionality of N/A in Eq. (3), the simultaneous reduction of N and m^* by the same factor will yield identical reflectivity values. Thus, the curve labeled $m^*=0.2m_e$ and $N=10^{20}$ cm^{-3} can also be marked $m^*=0.04m_e$ and $N=2\times10^{19}$ cm^{-3}. Thus, a smaller effective mass or higher-carrier concentration will shift the free-carrier plasma edge towards higher frequencies.

For the material with the short relaxation time, Fig. 9(b), the curves for $N=10^{16}$ cm^{-3} and $N=5\times10^{17}$ cm^{-3} are nearly superimposed with no measurable contribution from the free carriers. As the carrier concentration is increased to 10^{19} cm^{-3}, a broad plasma edge does develop, but lattice vibration effects are clearly observable even at $N=10^{20}$ cm^{-3}. For the same carrier densities, the overall effect of a shorter relaxation time is the broadening of the plasma edge and a more gradual decrease of the reflectivity as a function of frequency. Both sets of curves shown in Fig. 9(a) and 9(b) were calculated from the simple superposition of the lattice and free-carrier parameters, without consideration of plasmon-polaron effects.

ACKNOWLEDGMENTS

The authors wish to thank Dr. Wang of Sperry Rand Research Center and L. Bouthillette of Wentworth Institute for the electrical measurements. Their appreciation is also expressed to J. Dolan and R. Menko for their help in data evaluation and computation, and to R. M. Barrett for his continued support of this work.